Characterizing Temperature Anisotropy with a Decade of RISR-N Extreme Ion Heating Events

Aidan Thayer [1], Lindsay V Goodwin [1], William J Longley [1], Jean-Pierre St-Maurice [2, 3]

Email: at968@njit.edu

1- Center for Solar-Terrestrial Research, Department of Physics, New Jersey Institute of Technology, Newark, NJ, USA

2- Department of Physics and Engineering Physics, University of Saskatchewan, Saskatoon, SK, Canada

3- Department of Physics and Astronomy, University of Western Ontario, London, ON, Canada

Introduction

- Advanced modular incoherent scatter radars (AMISRs) are capable of taking volumetric measurements of plasma (ion and electron temperature, plasma density, and line-of-sight velocity)
- AMISRs like the Resolute Bay Incoherent Scatter Radar (RISR-N) located at 74.7 N, 94.9 W have been operational since 2011 in a variety of modes to understand the dynamics of the E and F region of the lower auroral zone
- During periods of intense geomagnetic activity, strong electric fields can cause temperatures in the F region to become anisotropic relative to the magnetic field due to a distortion in the O+ velocity distribution [3] [5].
- **The impact of temperature anisotropy during geomagnetic events is not currently corrected for in radar fitting routines or atmospheric models, and as such we would like to characterize its effects.**

Figure 1. Photo of Resolute Bay Incoherent Scatter Radar-North (RISR-N) (Photo Credit Craig Heinselman)

Methodology

- F-region plasma along the same magnetic field line will be subject to the same plasma dynamics and E x B drift, implying that closely overlapping radar look directions are observing the same processes at different aspect angles.
- F-region RISR-N observations between 2010-2020 were labelled as a heating event if: 1) the ion temperature exceeded 1000 K, 2) the electron temperature was less than 3000 K (indicating low/no precipitation), and 3) plasma density exceeded 1e10m-3 (indicating reliable data).
- If the Spearman correlation coefficient between two overlapping observations between 200 km and 400 km exceeded 0.7 (finding the appropriate 2-hour heating window using 15-minute rolling increments):
  1. The ion temperatures parallel and perpendicular to the magnetic field were calculated (Eqs. 1, 2) [3]. A three-point rolling average was applied to both calculated temperatures to reduce noise.
  2. Orthogonal distance regression was used to calculate $\beta_{\parallel 1} / \beta_{\perp 1}$ (Eq. 3)
  3. Assuming the neutral winds were negligible, v_i was calculated using the north and east components of the ion flow [2].
  4. $\beta_{\parallel 2}$ and $\beta_{\perp 2}$ were then fit for using orthogonal distance regression and used to generate $\beta_{\parallel 2} / \beta_{\perp 2}$ (Eq. 4).
  5. The two beta ratios are compared, and the individual beta parameters validated (Eq. 5) [4].
- This is repeated for several heating events of varying intensities.
- A case study is performed on a 9/12/2014 extreme heating event [1] where the ion temperature exceeded 3500 K, and there were no signatures of precipitation.

$$T_{\parallel} = \frac{T_{\phi_1} - T_{\perp}\sin^2(\phi_1)}{\cos^2(\phi_1)} \quad (1) \qquad \beta_* = \frac{2k_B(T_* - T_n)}{m_n|v_i - v_n|^2} \quad (4)$$

$$T_{\perp} = \frac{T_{\phi_2} - \frac{T_{\phi_1}\cos^2(\phi_2)}{\cos^2(\phi_1)}}{\sin^2(\phi_2) - \tan^2(\phi_1)\cos^2(\phi_2)} \quad (2)$$

$$\frac{\beta_{\parallel}}{\beta_{\perp}} = \frac{T_{\parallel} - T_n}{T_{\perp} - T_n} \quad (3) \qquad \frac{\beta_{\parallel} + 2\beta_{\perp}}{2} = 1 \quad (5)$$

Results

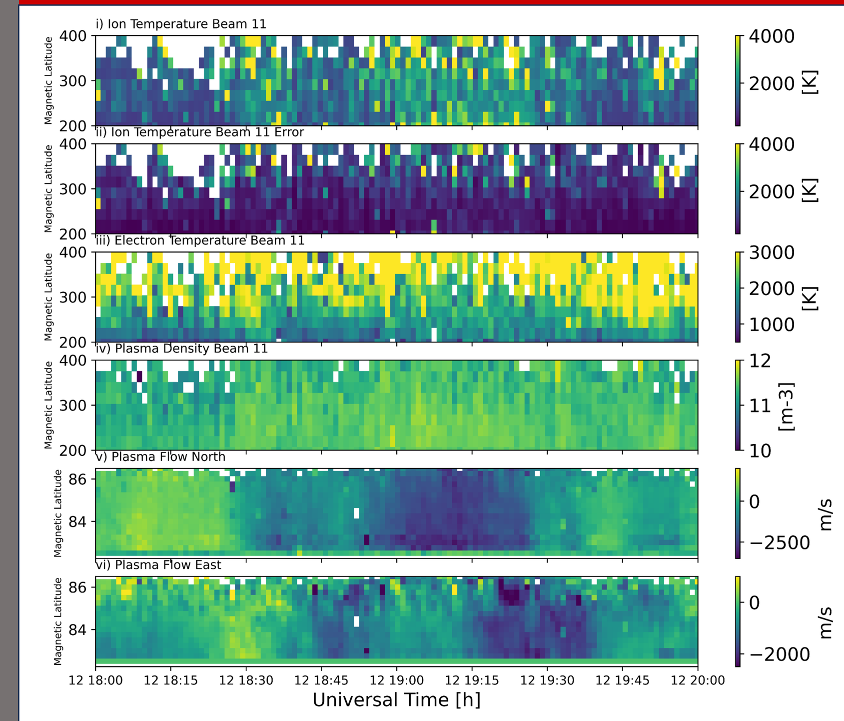

Figure 2: Range Time Intensity Plot of RISR-N Data from WorldDay 9/12/2014. Beam 11 with Azimuth Angle of 26 degrees, Elevation Angle of 90°, respectively.
Panel 1 is ion temperature, panel 2 is the error for the ion temperature, panel 3 is electron temperature, panel 4 is plasma density on a logarithmic scale, panel 5 is the northward velocity component, and panel 6 is the eastward velocity component

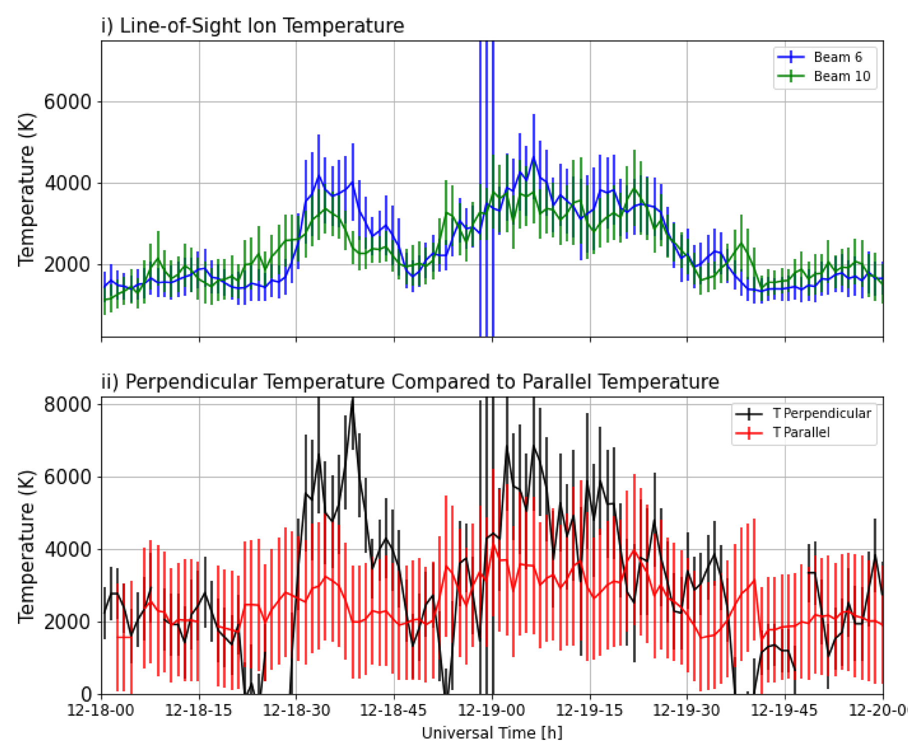

Figure 3: Top panel: Line-of-sight ion temperatures for Beams 6 and 10 at 238 km with one sigma error bars. Bottom panel: Corresponding perpendicular and parallel ion temperature. A three-point rolling average is applied. Line colors match corresponding variables in methodology.

Figure 4: All of the $\beta_{\parallel 1} / \beta_{\perp 1}$ and $\beta_{\parallel 2} / \beta_{\perp 2}$ are calculated for 1800 to 2000 UTC 9/12/14 for the nearest 4 range gates for altitudes between 200-400 km colored by the corresponding paired beam. Panels 1-9 are comparing each beam pair's $\beta_{\parallel 1} / \beta_{\perp 1}$ as a function of magnetic latitude, panels 10-18 are checking the ratio between $\beta_{\parallel 1} / \beta_{\perp 1}$ and $\beta_{\parallel 2} / \beta_{\perp 2}$, and panels 19-27 are checking the validity of Eq 5. by summing $\beta_{\parallel 2}$ and $2\beta_{\perp 2}$ and dividing by 2

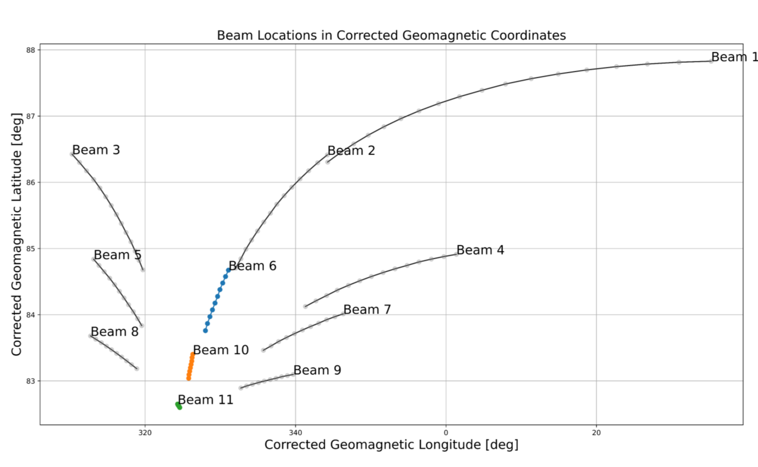

Figure 5: Beam Map of WorldDay Experiment as a function of latitude and longitude. In color are the beams shown in Figures 2-3

Results (cont.)

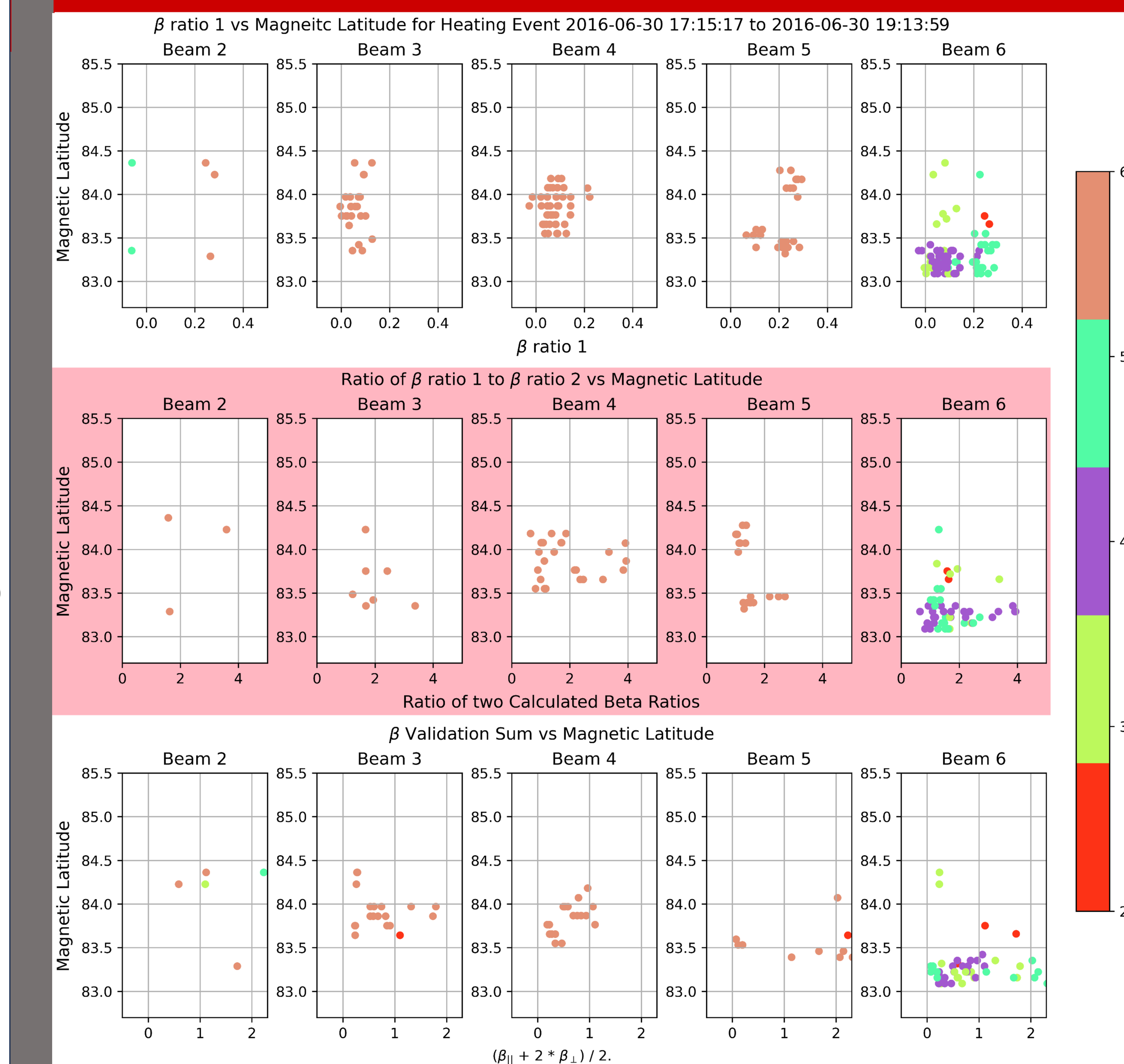

Figure 5: Just as in Figure 4, all of the $\beta_{\parallel 1} / \beta_{\perp 1}$ and $\beta_{\parallel 2} / \beta_{\perp 2}$ are calculated for 1715 to 1915 UTC 6/30/16 for the nearest 4 range gates for altitudes between 200-400 km colored by the corresponding paired beam. Note that this is a Calibration experiment and therefore only has 6 beams running, rather than World Day's 11, though this does mean lower signal to noise. Panels 1-5 are comparing each beam pair's $\beta_{\parallel 1} / \beta_{\perp 1}$ as a function of magnetic latitude, panels 6-10 are checking the ratio between $\beta_{\parallel 1} / \beta_{\perp 1}$ and $\beta_{\parallel 2} / \beta_{\perp 2}$, and panels 11-15 are checking the validity of Eq 5. by summing $\beta_{\parallel 2}$ and $2\beta_{\perp 2}$ and dividing by 2.

Discussion and Future Work

This method allows for calculating the degree of temperature anisotropy for both extreme and generally high intensity heating events measured by RISR-N at high latitudes, and we have demonstrated enough robustness through several validation methods to be confident in the results. As the intensity of the of the event decreases, our confidence in the Beta parameter decreases due to the lower correlations involved, but our initial fits from the high intensity event converge to $\beta_{\parallel} / \beta_{\perp} \approx 0.25 \pm 0.18$. With basic statistical filtering techniques and examining the physically incompatible (and unvalidated) fits for trends, the uncertainty in this ratio will decrease and allow more confidence in using this technique on a larger catalogue of events.

References & Acknowledgements

1- Clauer, C. R., Z. Xu, M. Maimaiti, J. M. Ruohoneimi, W. Scales, M. D. Hartinger, M. J. Nicolls, S. Kaeppler, F. D. Wilder, and R. E. Lopez (2016), Investigation of a rare event where the polar ionospheric reverse convection potential does not saturate during a period of extreme northward IMF solar wind driving, *J. Geophys. Res. Space Physics*, 121, 5422–5435, doi:10.1002/2016JA022557

2- Heinselman, C. J., and M. J. Nicolls (2008), A Bayesian approach to electric field and E-region neutral wind estimation with the Poker Flat Advanced Modular Incoherent Scatter Radar, *Radio Sci.*, 43, RS5013, doi:10.1029/2007RS003805.

3- Raman, R. S. V., St-Maurice, J. P., & Ong, R. S. B. (1981). Incoherent scattering of radar waves in the auroral ionosphere. *Journal of Geophysical Research*, *86*(A6), 4751–4762. https://doi.org/10.1029/ja086ia06p04751

4- St-Maurice, J.-., Hanson, W. B., & Walker, J. C. G. (1976). Retarding potential analyzer measurement of the effect of ion-neutral collisions on the ion velocity distribution in the auroral ionosphere. *Journal of Geophysical Research*, *81*(31), 5438–5446. https://doi.org/10.1029/ja081i031p05438

5- St-Maurice, J.-P., and R. W. Schunk (1979), Ion velocity distributions in the high-latitude ionosphere, *Rev. Geophys.*, 17(1), 99–134, doi:10.1029/RG017i001p00099.

Efforts by AT, LVG, and WJL are supported by the NSF under CEDAR award #2330254. The authors wish to thank Chirag Skolar for their personal correspondence. This material is based upon work supported by the Resolute Bay Observatory, which is a major facility funded by the National Science Foundation through cooperative agreement AGS-1840962 to SRI International. RISR-N data is available through the SRI International ISR Database (https://amisr.com/database/)